Chapter 4

SELF-ASSEMBLY OF ASYMMETRIC BRUSH BLOCK COPOLYMERS

ABSTRACT

Self-assembled structures of asymmetric brush block copolymers (BCPs) with polylactide (PLA) and polystyrene (PS) side chains were studied. The volume fractions of each block were varied in order to observe where morphological transitions took place. AFM and SEM imaging showed a transition from lamellar to a cylindrical-like morphology when the volume fraction of one of the blocks exceeded 70% for samples annealed by either thermal compression or controlled evaporation from tetrahydrofuran (THF). Drop-cast samples were analyzed via small-angle X-ray scattering (SAXS). They were found to be kinetically trapped in their initial morphologies that were best indexed to an undulating lamellar type structure, where the primary structure is a lamellar array, but with small regions possessing short-range hexagonal order.

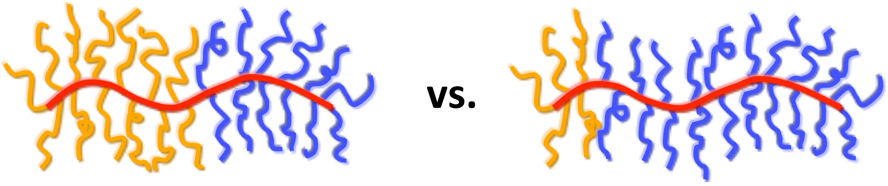

INTRODUCTION

Block copolymers (BCPs) have attracted tremendous interest from both academia and industry because of their ability to self-assemble into periodic structures with domain spacing ranging from 10 to 100 nm.[1–3] The incompatibility effects arising from the particular chemical structure of block copolymers give them a number of specific morphologies such as spheres, cylinders, lamellae, or gyroid, which leads to numerous technological applications.[4,5] For a noncrystalline A-B diblock copolymer, the bulk morphology is determined by Flory-Huggins parameter, χ, the total degree of polymerizaion, N, and volume fraction of each block, f. When χN exceeds the critical value for the order-disorder transition, the repulsive interactions between the blocks are strong enough for microphase separation to occur.[6] By increasing the asymmetry of the volume fractions of each block in a BCP, the morphology of the microdomains can be shifted from lamellar to hexagonally arranged cylinders to cubically ordered spheres.[6,7] The ability to control the morphology of BCPs is important to tuning the BCP properties for specific application. For example, for photonic materials, the morphology affects in how many dimensions light modes can be localized.[8,9]

Morphological transitions have been well studied for linear BCPs and have resulted in phase diagrams for a number of polymer systems. However, to the best of our knowledge, morphology transitions of brush BCPs have not yet been studied. This chapter describes our initial findings concerning where the morphology transitions of a polylactide (PLA)/polystyrene (PS) based brush BCP system take place.

SYNTHESIS OF ASYMMETRIC BRUSH BCPs

Asymmetric brush BCPs were synthesized in an analogous manner, as described in *Chapter 2*, using a sequential ruthenium-catalyzed ring-opening metathesis polymerization (ROMP) of PLA and PS based macromonomers (MMs).[10] The molar equivalences of the MMs were varied during the sequential ROMP in order to control the asymmetry of the blocks in the resulting brush BCP. Several series of asymmetric brush BCPs were synthesized, as shown in **Table 4-1**. Each series utilized different side chain lengths; within each series, the block length asymmetry was varied while maintaining approximately constant total degree of polymerization (DP). The form of the sample codes, $[g\text{-}S_x]_p\text{-}b\text{-}[g\text{-}LA_y]_q$, is the same as used in *Chapter 3,* where the subscripts x and y are the molecular weights of the side chains of each type (in units of one thousand), and subscripts p and q represent the degree of polymerization of each brush block.

Table 4-1. Sample codes and characteristics of asymmetric brush block copolymers.

Group	Sample codes	Total M_n [a] (× 10^3 g/mol)	PDI [a]	Total DP [b]	PLA% [b]	PS% [b]
I	[*g*-S$_{2.4}$]$_{56}$-*b*-[*g*-LA$_{2.4}$]$_{182}$	565	1.14	238	76	24
	[*g*-S$_{2.4}$]$_{64}$-*b*-[*g*-LA$_{2.4}$]$_{158}$	528	1.07	222	71	29
	[*g*-S$_{2.4}$]$_{118}$-*b*-[*g*-LA$_{2.4}$]$_{137}$	607	1.09	255	54	46
II	[*g*-S$_{4.3}$]$_{26}$-*b*-[*g*-LA$_{4.3}$]$_{174}$	868	1.07	194	87	13
	[*g*-S$_{4.3}$]$_{56}$-*b*-[*g*-LA$_{4.3}$]$_{160}$	934	1.06	209	74	26
	[*g*-S$_{4.3}$]$_{159}$-*b*-[*g*-LA$_{4.3}$]$_{48}$	895	1.09	204	23	77
	[*g*-S$_{4.3}$]$_{195}$-*b*-[*g*-LA$_{4.3}$]$_{24}$	943	1.06	216	11	89
III	[*g*-S$_{2.6}$]$_{332}$-*b*-[*g*-LA$_{2.5}$]$_{17}$	902	1.03	349	5	95
	[*g*-S$_{2.6}$]$_{314}$-*b*-[*g*-LA$_{2.5}$]$_{29}$	885	1.01	342	8	92
	[*g*-S$_{2.6}$]$_{313}$-*b*-[*g*-LA$_{2.5}$]$_{46}$	929	1.02	359	13	87
	[*g*-S$_{2.6}$]$_{343}$-*b*-[*g*-LA$_{2.5}$]$_{68}$	1060	1.02	411	17	83
	[*g*-S$_{2.6}$]$_{278}$-*b*-[*g*-LA$_{2.5}$]$_{73}$	905	1.05	351	21	79
	[*g*-S$_{2.6}$]$_{288}$-*b*-[*g*-LA$_{2.5}$]$_{95}$	988	1.05	383	25	75
	[*g*-S$_{2.6}$]$_{273}$-*b*-[*g*-LA$_{2.5}$]$_{117}$	1005	1.03	390	30	70
	[*g*-S$_{2.6}$]$_{264}$-*b*-[*g*-LA$_{2.5}$]$_{144}$	1049	1.02	408	35	65
IV	[*g*-S$_{4.7}$]$_{370}$-*b*-[*g*-LA$_{4.2}$]$_{19}$	1834	1.21	389	5	95
	[*g*-S$_{4.7}$]$_{364}$-*b*-[*g*-LA$_{4.2}$]$_{38}$	1888	1.18	402	10	90
	[*g*-S$_{4.7}$]$_{348}$-*b*-[*g*-LA$_{4.2}$]$_{63}$	1917	1.11	411	15	85
	[*g*-S$_{4.7}$]$_{332}$-*b*-[*g*-LA$_{4.2}$]$_{79}$	1910	1.10	411	19	81
	[*g*-S$_{4.7}$]$_{308}$-*b*-[*g*-LA$_{4.2}$]$_{102}$	1892	1.06	410	25	75
	[*g*-S$_{4.7}$]$_{283}$-*b*-[*g*-LA$_{4.2}$]$_{121}$	1853	1.06	404	30	70
	[*g*-S$_{4.7}$]$_{263}$-*b*-[*g*-LA$_{4.2}$]$_{143}$	1851	1.05	406	35	65
	[*g*-S$_{4.7}$]$_{268}$-*b*-[*g*-LA$_{4.2}$]$_{179}$	2028	1.06	447	40	60

[a] Determined by THF GPC using RI and MALLS detectors. [b] Degree of polymerization and mol percentages were determined by ^{1}H NMR and THF GPC (as described in *Chapter 2*).

RESULTS AND DISCUSSION

Samples from group I and group II were thermally annealed at 130 °C for 24 hours before being analyzed by atomic force microscopy (AFM). Samples from group I (**Figure 4-1**) showed that when the PS block was 46% of the whole brush BCP ([*g*-S$_{2.4}$]$_{118}$-*b*-[*g*-LA$_{2.4}$]$_{137}$), a lamellar structure was observed by AFM (**Figure 4-1C**). When the PS block was 29% ([*g*-S$_{2.4}$]$_{64}$-*b*-[*g*-LA$_{2.4}$]$_{158}$), a change in morphology was observed, where AFM images showed a structure that could be either a) part cylindrical and part lamellar, or b) cylindrical, where some of the cylinders are perpendicular to the surface and others are parallel to the surface (**Figure 4-1B**). At 24% PS incorporation in the brush BCP ($[g\text{-}S_{2.4}]_{56}\text{-}b\text{-}[g\text{-}LA_{2.4}]_{182}$), a uniform morphology was observed, indicating that the brush BCP may have self-assembled completely into a cylindrical structure (**Figure 4-1A**).

AFM images of $[g\text{-}S_{4.3}]_{26}\text{-}b\text{-}[g\text{-}LA_{4.3}]_{174}$ (13% PS) and $[g\text{-}S_{4.3}]_{56}\text{-}b\text{-}[g\text{-}LA_{4.3}]_{160}$ (26% PS) from group II (**Figure 4-2A-B**) showed a similar morphology to the 24% PS sample ($[g\text{-}S_{2.4}]_{56}\text{-}b\text{-}[g\text{-}LA_{2.4}]_{182}$) from group I, suggesting that these samples had a cylindrical morphology. However, when PLA was the major block in the brush BCPs, the AFM images were not as clear regarding their morphology. $[g\text{-}S_{2.4}]_{150}\text{-}b\text{-}[g\text{-}LA_{2.4}]_{48}$ (77% PS) showed some lamellar like structure, but not consistently throughout the sample (**Figure 4-2C**), and while ($[g\text{-}S_{2.4}]_{195}\text{-}b\text{-}[g\text{-}LA_{2.4}]_{24}$ (89% PS) displayed a structure that could be suggestive of a somewhat cylindrical morphology (**Figure 4-2D**), the image was not clear enough to make a conclusive conjecture. In order to determine the morphologies of the above-mentioned samples, more data, such as small angle X-ray scattering (SAXS), was required.

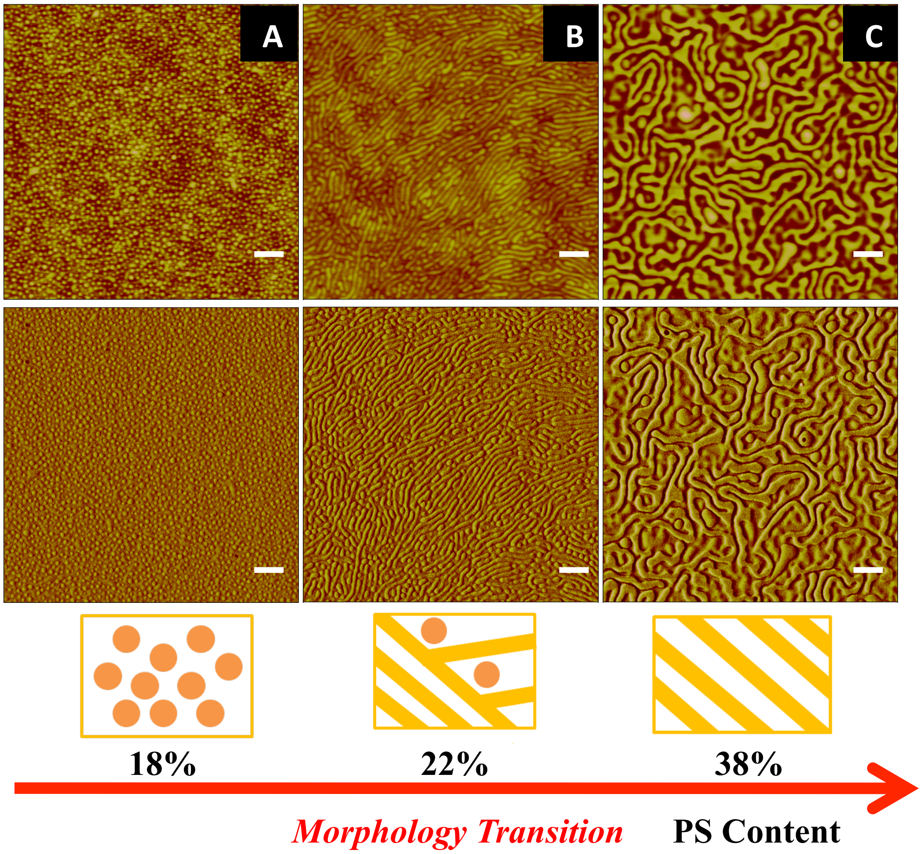

Figure 4-1. AFM height (first row) and phase (second row) images of A) $[g\text{-}S_{2.4}]_{56}\text{-}b\text{-}[g\text{-}LA_{2.4}]_{182}$; B) $[g\text{-}S_{2.4}]_{64}\text{-}b\text{-}[g\text{-}LA_{2.4}]_{158}$; and C) $[g\text{-}S_{2.4}]_{118}\text{-}b\text{-}[g\text{-}LA_{2.4}]_{137}$. Scale bar is 500 nm.

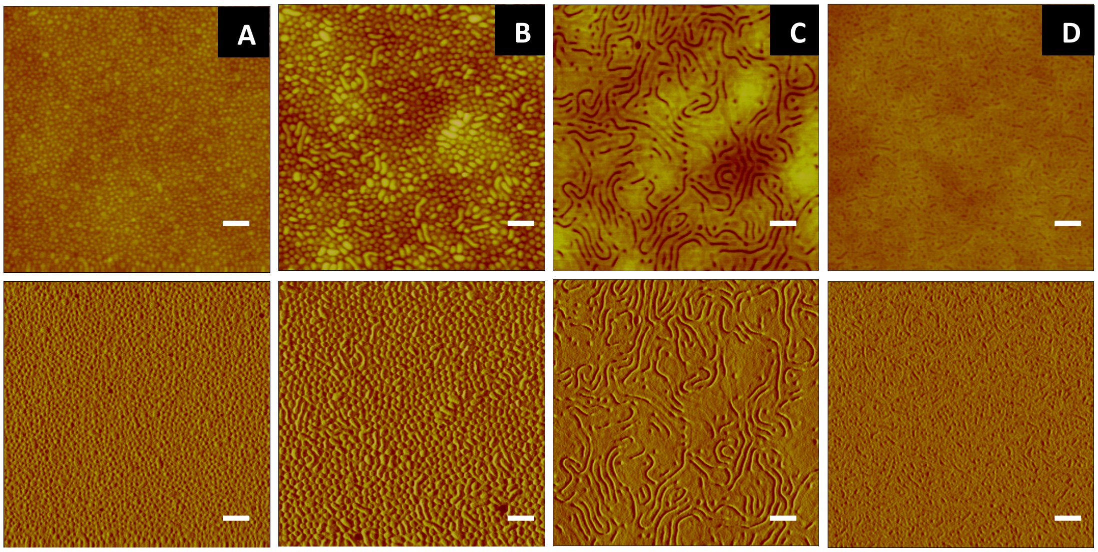

Figure 4-2. AFM height (first row) and phase (second row) images of A) $[g\text{-}S_{4.3}]_{26}\text{-}b\text{-}[g\text{-}LA_{4.3}]_{174}$; B) $[g\text{-}S_{4.3}]_{56}\text{-}b\text{-}[g\text{-}LA_{4.3}]_{160}$; C) $[g\text{-}S_{4.3}]_{159}\text{-}b\text{-}[g\text{-}LA_{4.3}]_{48}$; and D) $[g\text{-}S_{4.3}]_{195}\text{-}b\text{-}[g\text{-}LA_{4.3}]_{24}$. Scale bar is 500 nm.

In order to identify the volume fractions of PS/PLA where morphology transitions take place, brush BCPs from group III and group IV were drop-cast onto glass slides and analyzed via SAXS (**Figure 4-3**). These series had smaller increments of volume fractions, making it easier to identify where the morphology started to change. The SAXS profiles of the samples with highest degree of symmetry were best indexed to a lamellar morphology. As the asymmetry increased, the order of the samples decreased, as indicated by the reduced sharpness of the scattering peaks in the SAXS profiles and the reduced number of visible scattering peaks. However, some peaks appeared to be asymmetric, and other peaks were present only in some samples. This is more easily observed when the profiles are offset in order to align the first order scattering peak (**Figure 4-4**) (e.g. the presence/absence of a peak @ $q/q_o \sim 2.8$). This indicates that, in some of the samples, multiple different morphologies may be present, although with limited amount of order. We hypothesize that these results indicate that, since the drop-cast samples do not have adequate time to achieve thermodynamic equilibrium, these structures are kinetically trapped in the initial morphologies. These morphologies are best indexed to an undulating lamellar type structure where the primary structure is a lamellar array, but with small regions possessing short-range hexagonal order.

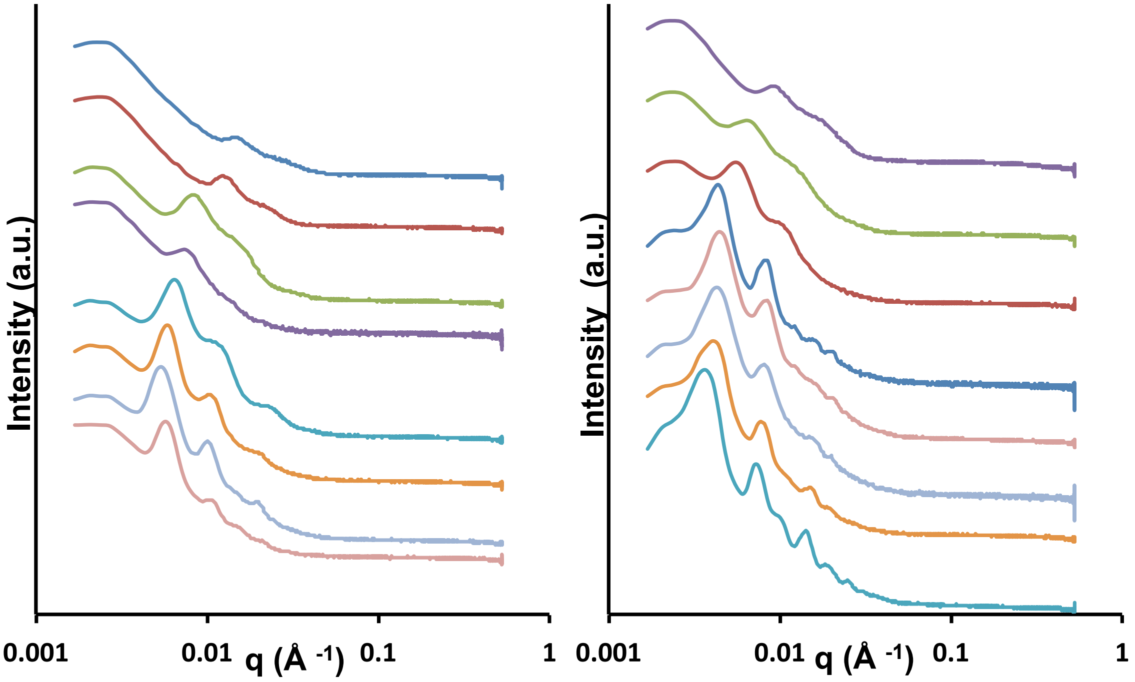

Figure 4-3. SAXS profiles of samples from group III (left) and group IV (right), where higher traces are of increased asymmetry.

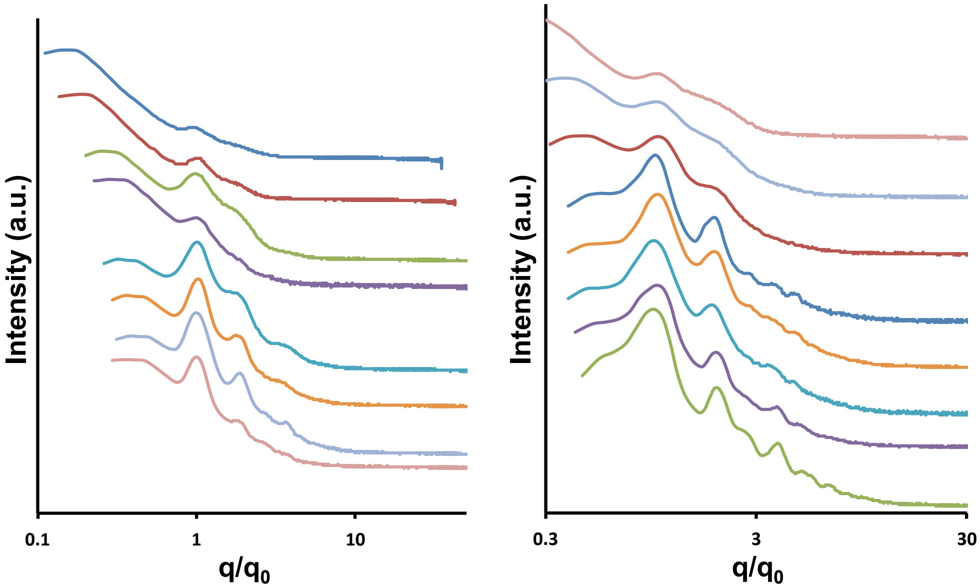

Figure 4-4. Offset SAXS profiles of samples from group III (left) and group IV (right), where higher traces are of increased asymmetry.

The group IV samples were also annealed via controlled evaporation from tetrahydrofuran (THF) on silica substrates, and thermal compression between two glass slides, before being subjected to scanning electron microscopy (SEM) imaging. For the samples annealed via controlled evaporation, it was clear that $[g\text{-S}_{4.7}]_{268}\text{-}b\text{-}[g\text{-LA}_{4.2}]_{179}$ (40% PS) and $[g\text{-S}_{4.7}]_{263}\text{-}b\text{-}[g\text{-LA}_{4.2}]_{143}$ (35% PS) gave lamellar structure (**Figure 4-5 A-B**). Meanwhile, $[g\text{-S}_{4.7}]_{282}\text{-}b\text{-}[g\text{-LA}_{4.2}]_{121}$ (30% PS) (**Figure 4-5C**) seemed to give a structure similar to the one observed in **Figure 4-1B** for $[g\text{-S}_{2.4}]_{64}\text{-}b\text{-}[g\text{-LA}_{2.4}]_{158}$, where it could be either a) part cylindrical and part lamellar, or b) cylindrical, in parts parallel and in parts perpendicular to the substrate. This provides further evidence that these brush BCPs seem to start undergoing some transition when one of the volume fractions is around 30%.

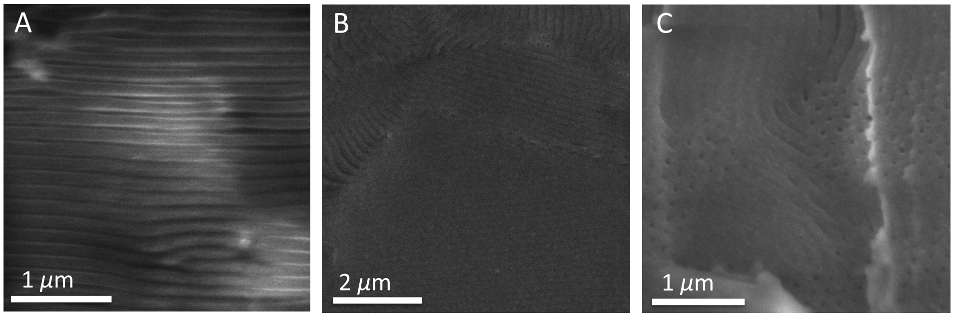

Figure 4-5. SEM images of a) $[g\text{-S}_{4.7}]_{268}\text{-}b\text{-}[g\text{-LA}_{4.2}]_{179}$; b) $[g\text{-S}_{4.7}]_{263}\text{-}b\text{-}[g\text{-LA}_{4.2}]_{143}$; and c) $[g\text{-S}_{4.7}]_{282}\text{-}b\text{-}[g\text{-LA}_{4.2}]_{121}$.

The thermally compressed samples did not give as clear morphologies. Nevertheless, there was a clear morphology change observed from $[g\text{-S}_{4.7}]_{263}\text{-}b\text{-}[g\text{-LA}_{4.2}]_{143}$ (35% PS) (**Figure 4-6A**) to $[g\text{-S}_{4.7}]_{282}\text{-}b\text{-}[g\text{-LA}_{4.2}]_{121}$ (30% PS) (**Figure 4-6B**). Other samples with more asymmetry showed somewhat similar structures that might suggest some cylindrical morphology for samples with up to 85% PS incorporation (**Figure 4-6C-D**). Clear SEM images were not obtained for other samples.

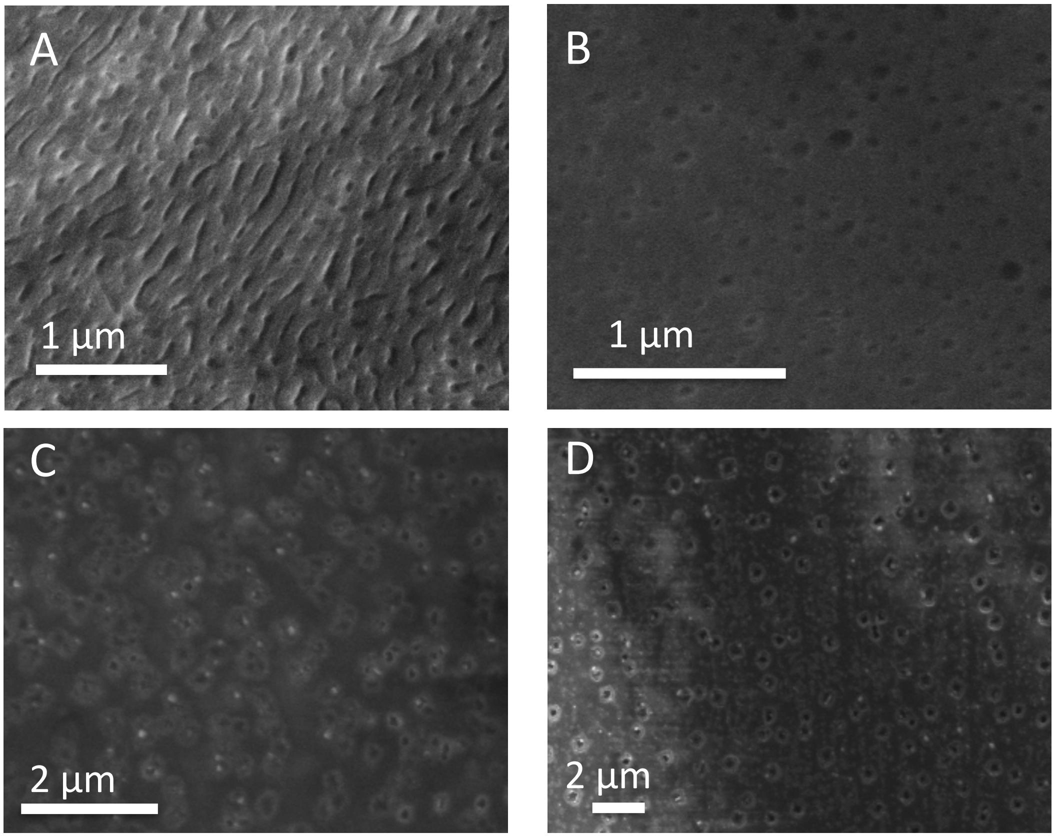

Figure 4-6. SEM images of a) $[g\text{-}S_{4.7}]_{263}\text{-}b\text{-}[g\text{-}LA_{4.2}]_{143}$; b) $[g\text{-}S_{4.7}]_{282}\text{-}b\text{-}[g\text{-}LA_{4.2}]_{121}$; c) $[g\text{-}S_{4.7}]_{332}\text{-}b\text{-}[g\text{-}LA_{4.2}]_{79}$; and d) $[g\text{-}S_{4.7}]_{348}\text{-}b\text{-}[g\text{-}LA_{4.2}]_{63}$.

CONCLUSIONS AND FUTURE DIRECTIONS

These results indicate that under thermal equilibrium, brush BCPs with similarly sized side chains undergo a morphology transition when the volume fraction of one of the blocks exceeds 70%. Asymmetric brush BCPs can also be kinetically trapped into a (undulating) lamellar morphology where the order of the sample decreases with increased asymmetry. In order to make more conclusive statements about the morphology transitions of asymmetric brush BCPs, it will be important to obtain SAXS data from samples that have achieved thermal equilibrium. Furthermore, it may prove valuable to explore the effect of the backbone length on the self-assembly of these macromolecules, as lower molecular weight brush BCPs have been shown to achieve thermal equilibrium more rapidly than those with higher molecular weights.[11]

REFERENCES:

(1) Bates, F. S.; Hillmyer, M. A.; Lodge, T. P.; Bates, C. M.; Delaney, K. T.; Fredrickson, G. H. *Science* **2012**, *336*, 434.

(2) Bates, F. S.; Fredrickson, G. H. *Annu. Rev. Phys. Chem.* **1990**, *41*, 525.

(3) Hamley, I. W. *The Physics of Block Copolymers*; Oxforrd University Press: New York, 1998.

(4) Segalman, R. A. *Mater. Sci. Eng. R Rep.* **2005**, *48*, 191.

(5) Tsui, O. K. C.; Russell, T. P. *Polymer Thin Films*; World Scientific: Singapore, 2008.

(6) Kim, H.-C.; Park, S.-M.; Hinsberg, W. D. *Chem. Rev.* **2010**, *110*, 146.

(7) Grubbs, R. B. *J. Polym. Sci. Part A Polym. Chem.* **2005**, *43*, 4323.

(8) Edrington, A. C.; Urbas, A. M.; DeRege, P.; Chen, C. X.; Swager, T. M.; Hadjichristidis, N.; Xenidou, M.; Fetters, L. J.; Joannopoulos, J. D.; Fink, Y.; Thomas, E. L. *Adv. Mater.* **2001**, *13*, 421.

(9) Joannopoulos, J. D. *Photonic Crystals: Molding The Flow of Light*; Princeton University Press, 2008.

(10) Sveinbjörnsson, B. R.; Weitekamp, R. A.; Miyake, G. M.; Xia, Y.; Atwater, H. A.; Grubbs, R. H. *Proc. Natl. Acad. Sci. USA* **2012**, *109*, 14332.

(11) Gu, W.; Huh, J.; Hong, S. W.; Sveinbjornsson, B. R.; Park, C.; Grubbs, R. H.; Russell, T. P. *ACS Nano* **2013**, *7*, 2551.